JOURNAL OF VIROLOGY, May 1997, p. 3407–3414 Vol. 71, No. 5
0022-538X/97/$04.00+0

Mutant Human Immunodeficiency Virus Type 1 Genomes with Defects in RNA Dimerization or Encapsidation

JARED L. CLEVER AND TRISTRAM G. PARSLOW*

Departments of Pathology and of Microbiology and Immunology, University of California, San Francisco, California 94143

Received 18 November 1996/Accepted 23 January 1997

Retrovirus particles each contain two copies of the viral genome in the form of a noncovalently linked RNA dimer. Earlier studies have mapped a *cis*-acting region near the 5′ end of the human immunodeficiency virus type 1 (HIV-1) genome, termed the ψ locus, which appears essential for initiation of genomic dimerization, as well as for interactions with the HIV-1 Gag protein that are thought to target the RNA into nascent virions. This HIV-1 ψ locus is proposed to be organized in four independent RNA stem-loops; at least three (SL1, SL3, and SL4) contain binding sites for Gag, and one of these (SL1) is implicated in dimer initiation through a kissing-loop mechanism. In this study, we have created HIV-1 proviruses containing ψ mutations that affect in vitro Gag binding, RNA dimerization, or both, and we have characterized the effects of these mutations on viral assembly and infectivity by using a single-step infectious assay. We find that various mutations which eliminate the Gag binding sites in SL1 or SL3 produce marked defects in genomic RNA packaging and viral infectivity. In each case, the reduced genomic content of the mutant virions is associated with an increased content of spliced viral transcripts, suggesting that both SL1 and SL3 contribute to the discrimination between spliced and unspliced RNAs. The structures, but not the specific sequences, of the SL1 and SL3 stems appear critical for RNA packaging. Disruption of the stem or deletion of SL1 also results in abnormal genomic dimerization, as assessed by nondenaturing gel electrophoresis of virion-derived RNA. Virions carrying less extensive mutations in the SL1 loop that are known to prevent in vitro dimerization have impaired infectivity despite normal virion RNA content. This suggests that RNA dimerization is not a prerequisite for genomic packaging but instead serves an independent function in the retroviral infectious cycle.

The process by which retroviral genomic RNA is assimilated into virion particles as they form is known as packaging, or encapsidation (recently reviewed in reference 6). The key events of encapsidation take place in the cytoplasm of an infected cell, where each nascent virion selectively incorporates two copies of the full-length viral genomic RNA while generally excluding cellular RNAs and spliced viral transcripts. Within the mature virion that results, these two genomic RNA strands are typically found to associate noncovalently with each other in parallel as a stable RNA dimer, but it is not known whether these dimers form before, during, or after encapsidation.

Genetic studies of several retroviruses, including human immunodeficiency virus type 1 (HIV-1), have helped to identify the requirements for efficient and selective RNA packaging. Such studies have revealed, for example, that packaging specificity is determined largely by one or two zinc finger elements and flanking basic residues in the nucleocapsid domain of the Gag protein: mutations in this region can abolish encapsidation (1, 13, 17, 33), and replacing nucleocapsid sequences from one virus with those of another can enable efficient packaging of a heterologous genome (9). Retroviral packaging also depends upon a type of *cis*-acting RNA element called a packaging signal, or ψ site, which generally maps to a region of a few hundred bases near the 5′ end of the genome of a given virus, close to both the major 5′ splice donor and the start codon of *gag* (20, 24, 25). Such ψ elements are, by definition, necessary for encapsidation, and in certain cases they are also sufficient to target an RNA into nascent virions of the corresponding virus (6). Interestingly, the location of the typical ψ locus also coincides with the most stable point of interstrand binding in the genomic RNA dimers of many retroviruses (3, 4, 29)—an observation which has long suggested that the processes of RNA dimerization and encapsidation might be mechanistically linked. It has been difficult to evaluate this possibility satisfactorily, however, largely because the molecular features and interactions involved in these two processes were not precisely known.

Recent in vitro analyses of the HIV-1 ψ locus have shed new light on its role in packaging and dimer formation. First, several laboratories have evaluated the conformation of HIV-1 ψ RNA by sequence analysis and nuclease accessibility mapping (2, 10, 19, 34); based on such data, we have proposed (10) a working model of the ψ locus that comprises four RNA stem-loops, designated SL1 to SL4 (Fig. 1A). Second, bacterially expressed HIV-1 Gag or nucleocapsid proteins have been shown to bind specifically to this ψ RNA (7, 8, 10, 34), with SL1, SL3, and SL4 each providing independent, high-affinity binding sites (10). It appears likely that similar Gag-ψ interactions occur within infected cells and play a key role in the encapsidation process. Finally, synthetic RNA oligonucleotides corresponding to the HIV-1 ψ sequence have been found to dimerize spontaneously in solution (12, 26). Such in vitro RNA dimerization is highly sequence specific, occurs more rapidly in the presence of Gag (12, 36), and is absolutely dependent on sequences in SL1, including a highly conserved 6-base palindrome (GCGCGC) in the SL1 loop. The latter observations have given rise to a "kissing-loop" model for HIV-1 RNA dimer initiation (23, 27, 32, 35), in which two genomic strands are proposed to interact first through base pairing between loop palindromes, possibly followed by

* Corresponding author. Mailing address: Department of Pathology, Box 0506, University of California, San Francisco, CA 94143. Phone: (415) 476-1015. Fax: (415) 476-9672. E-mail: parslow@cgl.ucsf.edu.

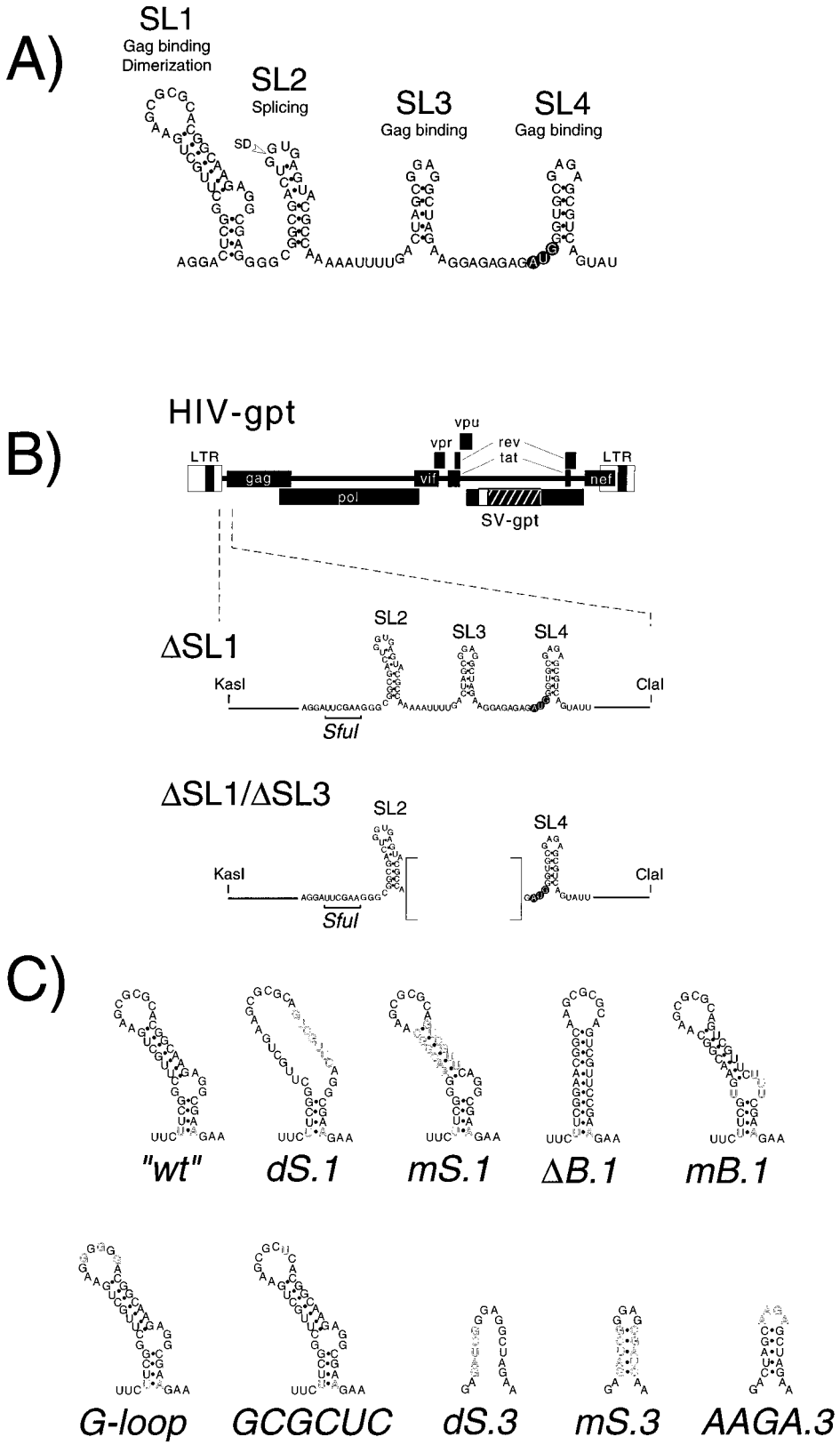

FIG. 1. (A) Working model of the HIV-1 ψ region (nt 693 to 811). Summarized are the results of previous studies which have shown that SL1, SL3, and SL4 each contain high-affinity Gag binding sites, while SL1 is necessary for initiating in vitro RNA dimerization. The major 5′ splice donor (SD) and the *gag* start codon are indicated (white lettering). (B) HIV-gpt provirus used in these studies, and the locations of deletions in ΔSL1 and ΔSL1/ΔSL3. The ΔSL3 construct was made by subcloning the "wild-type" SL1 sequence into ΔSL1/ΔSL3; therefore, both ΔSL1/ΔSL3 and ΔSL3 contain the identical deletion of SL3 and adjacent flanking nucleotides. (C) Point mutants tested in this study. Note that the only nucleotide alterations made in these proviruses are indicated with open lettering.

isomerization of the two SL1 stems to form an interstrand duplex (reference 11 and references therein). Together, such in vitro findings have helped to define the precise requirements for Gag binding and dimer formation, and they suggest approaches to manipulating those activities in vivo. The present study was designed to test and exploit these findings by creating live HIV-1 virions that would be expected to exhibit selective defects in dimerization or in encapsidation, based on data from the in vitro RNA dimerization and Gag binding assays.

MATERIALS AND METHODS

Cell culture. Human osteosarcoma (HOS) and 293T cells were cultured at 37°C under 5% CO_2 in Dulbecco's modified Eagle's medium containing 4.5 g of glucose per liter, 100 U of penicillin G per ml, 0.1 mg of streptomycin sulfate per ml, and 10% fetal calf serum.

Vector construction. All ψ site mutations were introduced into the previously described HIV-gpt vector (22, 30) (a gift of N. Landau and D. Littman). The amphotropic murine leukemia virus Env expression vector has also been previously described (30). The HIV-1 provirus containing a precise deletion of SL1 (nucleotides [nt] 697 to 731), replaced with a unique *Sfu*I restriction enzyme site, was created by exchanging the unique *Kas*I (nt 637)-*Cla*I (nt 829) fragment of HIV-gpt with the equivalent fragment from the previously described ΔSL1 construct (11). Mutant forms of SL1 were then subcloned into the *Sfu*I site of the ΔSL1 proviruses with overlapping synthetic oligonucleotides with *Sfu*I ends (Fig. 1). This cloning strategy re-creates the SL1 sequence, except that the first base pair in the stem is changed from a C · G to a U · A in all SL1 mutants, with no additional residues added unless otherwise noted. Mutations in SL3 were created by oligonucleotide-directed mutagenesis (21) of the unique *Kas*I-*Cla*I fragment of HIV-1 subcloned into pBluescript II KS^+ (pBS/KS^+; Stratagene), after which DNAs were sequenced to confirm the presence of the expected mutations. These *Kas*I-*Cla*I fragments were then subcloned into the HIV-gpt vector cut with the same restriction enzymes. Constructs for in vitro transcription of antisense riboprobes, used in the RNase protection assays, were made by subcloning the *Kpn*I-*Cla*I fragment of wild-type or mutant HIV-gpt into pBS/KS^+ cut with the same enzymes. Prior to in vitro transcription with T7 RNA polymerase, plasmids were linearized with *Bsp*EI (nt 309). Radiolabelled transcripts were prepared exactly as described previously (10).

Virus production and infectivity assays. All virions used in these studies consisted of HIV-1 core particles (strain HXB2) pseudotyped with the amphotropic murine leukemia virus Env protein (22, 30). Viral stocks were prepared from transient calcium phosphate cotransfection of 293T cells at 50% confluency grown in T75 flasks (Corning) with 15 μg each of Env expression and provirus-containing vectors. After 12 h, the supernatants were discarded and the cells were refed with 20 ml of fresh medium. Viral stocks were harvested 48 h posttransfection and filtered through 0.45-μm syringe filters (Nalgene) before being stored at −70°C or used immediately. Infectivity assays were performed in duplicate by serial dilutions of the viral supernatants. HOS cells, grown in six-well plates at approximately 30% confluency, were infected for 90 min at 37°C with virus contained in 0.5 ml of medium plus 8 μg of Polybrene per ml before the addition of 1 ml of medium. After 24 h at 37°C, the supernatants were replaced with 1.5 ml of selection medium (22) containing 25 μg of mycophenolic acid per ml. The medium was changed every 3 or 4 days, and colonies were fixed and stained with crystal violet after about 12 to 15 days under selection as previously described (22).

Virus quantitation, immunoblotting, and reverse transcriptase assays. The concentration of viral antigen (p24) in the stocks was determined by an enzyme immunoassay as recommended by the manufacturer (Coulter-Immunotech). All p24 concentrations are an average of two different dilutions of the viral stocks within the linear range of the standard curve. For immunoblotting, viral supernatants containing approximately 75 ng of p24 were pelleted through a 0.2-ml 20% (wt/vol) sucrose cushion in a 1.5-ml microcentrifuge tube at 40,000 × *g* for 2 h at 4°C, after which the pellet was resuspended in 10 μl of 2× sodium dodecyl sulfate (SDS) sample buffer and heated to 100°C for 3 min. Samples were electrophoresed on SDS–12.5% (wt/vol) polyacrylamide gels, electroblotted onto Hybond C-Extra membranes (Amersham), blocked for 30 min in BLOTTO (5% [wt/vol] nonfat dry milk plus 0.1% [vol/vol] Tween 20 in phosphate-buffered saline [PBS]), and then probed overnight at 25°C with a 1:10,000 dilution of pooled patient antisera (a gift of A. Leavitt, University of California San Francisco). After extensive washing in 0.1% Tween 20 in PBS, the membranes were incubated for 1 h at 25°C with a 1:5,000 dilution of sheep anti-human immunoglobulin G antibody conjugated to horseradish peroxidase (Amersham). After being washed, the membranes were treated with enhanced chemiluminescence substrate (Amersham) and exposed to film. Reverse transcriptase assays were performed in duplicate on virions pelleted from 0.5 ml of viral stocks at 25,000 × *g* for 1 h at 4°C. The pellets were resuspended in 50 μl of 50 mM Tris-HCl (pH 7.6)–10 mM dithiothreitol–10 mM $MgCl_2$, 0.05% Nonidet P-40–48 μg of poly(rA) (Pharmacia) per ml–12 μg of oligo(dT) (Clontech) per ml–40 μCi of [*methyl*-^{3}H]TTP (Amersham) per ml–10 μM dTTP and then incubated at 37°C for 2 h. The reaction mixtures were spotted onto DE-81 filter paper (Whatman), dried, and washed five times with 2× SSC (1× SSC is 0.15 M NaCl plus 0.015 M sodium citrate [pH 7.0]), once with water, and once with ethanol; the filters were then dried and quantitated by liquid scintillation counting.

RNase protection assays. Viral stocks (10.5 ml) were layered onto a 1-ml 20% sucrose cushion (in PBS) and centrifuged at 150,000 × *g* in an SW41 rotor (Beckman) for 1.5 h at 4°C. Viral pellets were resuspended in 0.1 ml of PBS, and an aliquot was removed to determine the p24 concentration as described above. Virions were disrupted by the addition of virus lysis buffer (50 mM Tris-HCl [pH 7.6], 10 mM EDTA, 1% SDS, 100 mM NaCl, 50 μg of tRNA/ml, 100 μg of proteinase K/ml) for 30 min at 25°C. After two phenol-chloroform extractions and one chloroform extraction, viral RNAs were precipitated with ethanol. Cytoplasmic RNAs were prepared from 293T cells 48 h posttransfection by resuspending the cell pellets in 0.4 ml of cell lysis buffer (10 mM Tris-HCl [pH 7.6], 140 mM NaCl, 1.5 mM $MgCl_2$, 0.5% Nonidet P-40, 1 mM dithiothreitol, 100 U of RNase inhibitor [Boehringer Mannheim]) by brief vortexing and then were incubated for 5 min on ice and microcentrifuged at 4°C for 10 min. The supernatants were treated with 0.2% SDS–125 μg of proteinase K per ml at 37°C for 30 min and then subjected to phenol-chloroform extraction and ethanol precipitation as described above. Viral and cytoplasmic RNA preparations were treated with 1.0 U of RQ1 RNase-free DNase (Promega) plus 10 U of RNase inhibitor in 0.1 ml for 30 min at 37°C and then subjected to phenol-chloroform extraction and ethanol precipitation to remove any plasmid DNA contamination. Amounts of viral RNAs were quantitated by an RNase protection assay (RPA II) as recommended by the manufacturer (Ambion). For virion-derived RNAs, the amount of RNA equivalent to 100 ng of pelleted p24 was annealed to an excess of ^{32}P-labelled riboprobe (10^5 cpm, ca. 200 pg). For cytoplasmic RNAs, approximately 1/20 to 1/40 of the RNA isolated from one T75 flask of 293T cells was used. Because transfection efficiencies varied, we quantified the ratios of genomic to spliced viral RNAs, rather than the absolute amounts of these RNAs, for comparisons among mutants (Table 1). The protected fragments were electrophoresed on denaturing 5% polyacrylamide–8 M urea sequencing gels and subjected to autoradiography. Radioactivity in the various bands was quantitated with a Molecular Dynamics PhosphorImager.

Extraction of RNA dimers and nondenaturing Northern blotting. Viral stocks (40 ml) were centrifuged in an SW28 rotor (Beckman) at 76,000 × *g* for 2 h at 4°C. Viral pellets were disrupted in virus lysis buffer, and RNA was extracted as above. Pelleted RNAs were resuspended in 10 mM Tris-HCl (pH 7.6)–1 mM EDTA–1.0% SDS–100 mM NaCl before being split and heated in parallel to the various temperatures indicated for 10 min, after which the samples were electrophoresed on 1% agarose gels in Tris-borate-EDTA buffer (TBE) at 4°C. Nondenaturing Northern blotting was performed essentially as previously described (14). After capillary blotting, membranes (N^+ nylon; Amersham) and RNAs were cross-linked with UV light and hybridized with 10^6 cpm of the wild-type riboprobe used in the RNase protection assays per ml. The membranes were washed extensively in 0.1× SSC–0.5% SDS at 68°C before being subjected to autoradiography.

RESULTS

We previously described RNA oligonucleotides representing several mutant forms of the HIV-1 ψ locus that had specific defects in Gag protein binding or RNA dimerization as measured by in vitro assays (10, 11). For the present study, we introduced these and other mutations into a cloned HIV provirus to test their effects in vivo. All studies were conducted with the parental vector pHIV-gpt (22, 30), which comprises a full-length provirus of HIV-1 (HXB2) in which a portion of the viral *env* coding sequence has been replaced by a bacterial xanthine-guanine phosphoribosyltransferase (*gpt*) drug resistance gene under the control of a simian virus 40 promoter (Fig. 1B). When transiently transfected into cultured 293T cells, this vector mimics most activities of an HIV-1 provirus, including the production of Gag polyprotein and genomic transcripts, but it is unable to produce infectious particles because it lacks a functional *env* gene. When pHIV-gpt is cotransfected along with a second plasmid that encodes a murine amphotropic Env protein, however, pseudotyped virions that contain the HIV-gpt genomic RNA are assembled and released into the culture supernatant, from which they can be harvested and assayed to determine their RNA contents. In addition, these pseudotyped particles can be used to infect HOS cell cultures. Although such virions can support only a single round of infection, each infected HOS cell becomes gpt^+ and acquires the ability to form a colony in the presence of mycophenolic acid;

TABLE 1. Characterization of viral mutants used in this study

Construct	Mean p24 concn (ng/ml)[a]	% Particle-associated p24[b]	RT/p24 ratio[c]	% Genomic RNA content[d]	Ratio of genomic/spliced RNA in:		Infectivity (CFU/ng of p24)[g] in:	
					Virions[e]	Cytoplasm[f]	Expt 1	Expt 2
HIV-gpt	307	63	100	100	10/1	2.1/1	2,330	2,901
ΔSL1	221	60	84	19	1/1	2.0/1	243	—[h]
ΔSL3	126	62	101	12	0.8/1	1.8/1	175	154
ΔSL1/ΔSL3	173	51	117	5	0.4/1	1.9/1	126	—
"wt"	394	61	98	91	9/1	1.7/1	2,670	—
dS.1	246	49	70	11	1/1	2.4/1	277	—
mS.1	207	48	65	42	4/1	2.1/1	1,748	—
G-loop	259	52	92	83	3/1	2.1/1	388	—
GCGCUC	217	36	78	42	2/1	—	355	—
ΔB.1	91	39	74	14	2/1	—	252	—
mB.1	237	32	57	18	1/1	—	180	—
dS.3	169	72	102	42	1/1	ND[i]	—	189
mS.3	298	54	92	105	7/1	ND	—	1,617
AAGA.3	275	70	89	81	15/1	ND	—	997

[a] Mean p24 concentration in viral stocks from at least three independent transfections.
[b] Percentage of p24 which was recovered from viral stocks after pelleting through a 20% sucrose cushion; data from one representative experiment.
[c] Reverse transcriptase (RT) activity in viral stocks relative to the concentration of p24, with the ratio from HIV-gpt as 100; data from one representative experiment.
[d] Percentage of genomic RNA in virions relative to the parental HIV-gpt virus; data from one representative experiment.
[e] Ratio of genomic to spliced viral RNAs extracted from pelleted virions (expressed as counts per minute in the genomic band/counts per minute in the spliced band); data from one representative experiment.
[f] Ratio of genomic to spliced viral RNAs extracted from the cytoplasm of transfected cells (expressed as in footnote *e*); data from one representative experiment.
[g] Infectivity, based on the CFU per nanogram of p24, from two representative experiments.
[h] —, value not determined in the experiment shown.
[i] ND, value not determined.

the colony-forming titer of a given mutant thus provides a quantitative measure of its infectivity in vivo.

Cleavage of pHIV-gpt with *Kas*I and *Cla*I excises a unique 192-bp region that encompasses the entire ψ locus; we constructed mutant viruses by replacing this region with synthetic oligonucleotides carrying specific deletions or point mutations, as illustrated in Fig. 1B and C. Most of the mutations tested in this study were confined to the SL1 or SL3 elements of ψ, so as to minimize possible effects on the major splice donor site in SL2 or the *gag* start codon at the base of SL4. Supernatants of 293T cells transfected with these mutants typically contained 100 to 400 ng of HIV p24 protein per ml 48 h after transfection, a range comparable to the 300 ng/ml obtained with pHIV-gpt (Table 1). In every case, 32 to 72% of this extracellular p24 appeared to be associated with viral particles, as judged by its ability to sediment through sucrose on centrifugation, and particle-associated reverse transcriptase activities of the mutants were also comparable to those of the parent vector (Table 1). Western blots of sucrose-pelleted virions, probed with polyclonal human HIV-1 antisera, confirmed the variability in viral protein expression among mutants but indicated that none of the mutants we tested significantly affected the qualitative pattern of HIV protein synthesis or processing (Fig. 2).

The expression and encapsidation of viral RNA by these mutants was evaluated by an RNase protection assay (Fig. 3A). Total RNA was extracted from sucrose-purified virion particles and from the cytoplasm of transfected 293T cells for each of the mutants, and equivalent amounts of virion-derived RNAs were then hybridized to an excess of complementary RNA probe that recognized 5′ viral RNA sequences spanning the major splice donor site. Probes were designed for each mutant to generate three discrete protected fragments when the RNA hybrids were treated with RNase: the largest corresponded to full-length genomic RNA; the second largest corresponded to spliced RNA; and the smallest corresponded to the 3′ long terminal repeat (LTR) sequence, which served as an internal control for total viral RNA concentration (an additional band, corresponding to proviral DNA contamination, was not detectable in any sample). Representative results are shown in Fig. 3B and summarized in Table 1 and Fig. 4A. All tested mutants yielded similar ratios of genomic to spliced viral transcripts in the cytoplasm, typically producing steady-state concentrations of genomic RNA that were 2-fold higher than those of spliced viral RNA (range, 1.7- to 2.4-fold) at 48 h posttransfection. Although the relative amounts of viral RNAs in the cytoplasmic fractions varied among the different mutants within an experiment, probably as a result of variations in transfection efficiencies (Fig. 3B), the ratio of genomic to spliced RNAs was found to be very consistent among the mutants over multiple experiments (Table 1). None of the mutants had consistently reduced viral RNA expression or splicing, as observed in multiple experiments (data not shown).

The quantity of genomic RNA packaged into virions, by contrast, varied widely among mutants. In particular, deletion of either SL1 alone (construct ΔSL1) or of SL3 and adjacent flanking sequences (construct ΔSL3) reduced genomic pack-

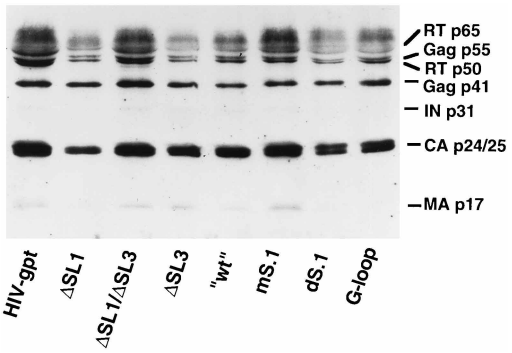

FIG. 2. Immunoblot of selected viral pellets probed with pooled patient anti-HIV-1 sera. The locations of major virion core proteins are indicated.

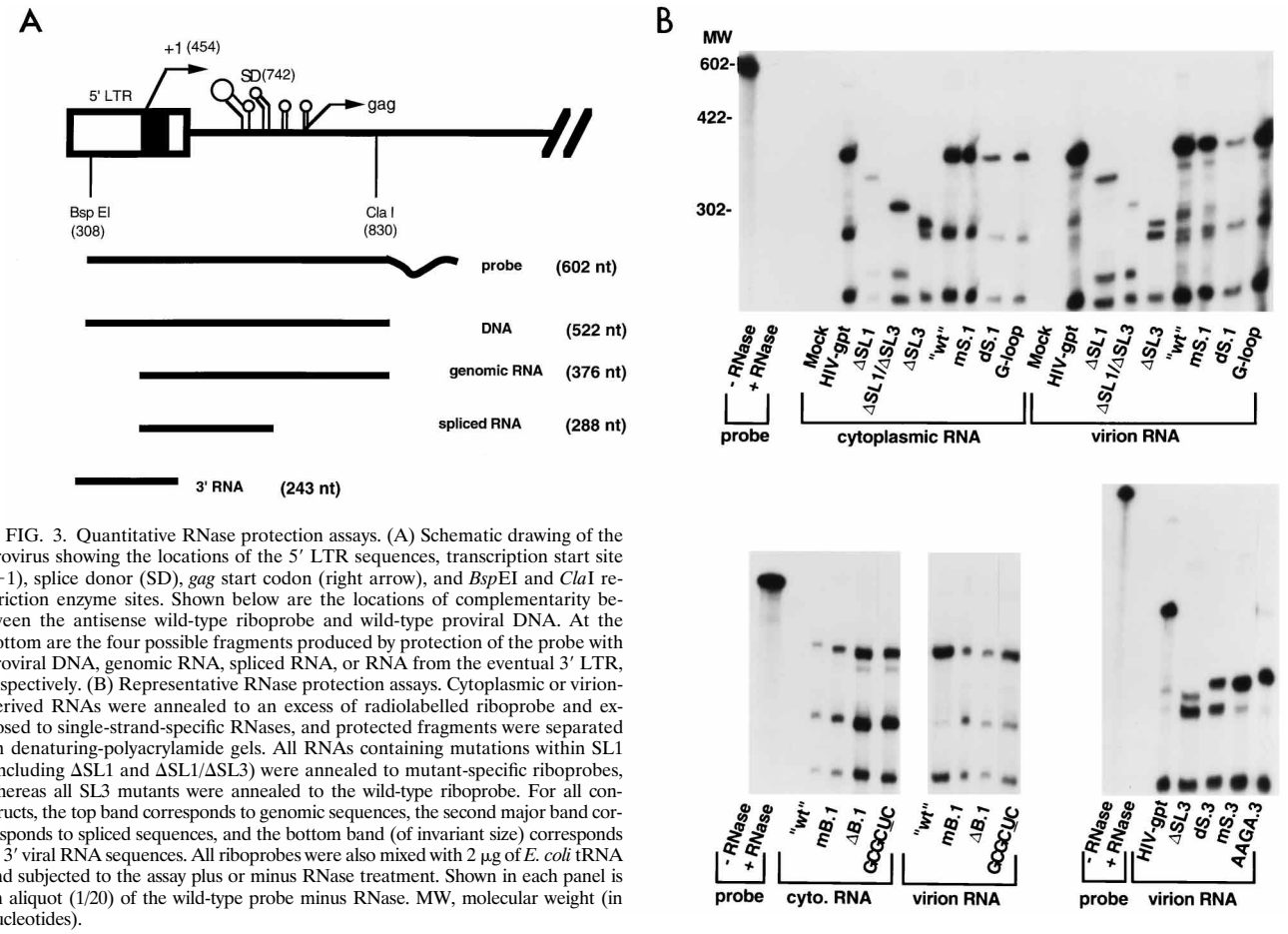

FIG. 3. Quantitative RNase protection assays. (A) Schematic drawing of the provirus showing the locations of the 5′ LTR sequences, transcription start site (+1), splice donor (SD), *gag* start codon (right arrow), and *Bsp*EI and *Cla*I restriction enzyme sites. Shown below are the locations of complementarity between the antisense wild-type riboprobe and wild-type proviral DNA. At the bottom are the four possible fragments produced by protection of the probe with proviral DNA, genomic RNA, spliced RNA, or RNA from the eventual 3′ LTR, respectively. (B) Representative RNase protection assays. Cytoplasmic or virion-derived RNAs were annealed to an excess of radiolabelled riboprobe and exposed to single-strand-specific RNases, and protected fragments were separated on denaturing-polyacrylamide gels. All RNAs containing mutations within SL1 (including ΔSL1 and ΔSL1/ΔSL3) were annealed to mutant-specific riboprobes, whereas all SL3 mutants were annealed to the wild-type riboprobe. For all constructs, the top band corresponds to genomic sequences, the second major band corresponds to spliced sequences, and the bottom band (of invariant size) corresponds to 3′ viral RNA sequences. All riboprobes were also mixed with 2 μg of *E. coli* tRNA and subjected to the assay plus or minus RNase treatment. Shown in each panel is an aliquot (1/20) of the wild-type probe minus RNase. MW, molecular weight (in nucleotides).

aging to 19 or 12%, respectively, of the level observed with HIV-gpt. Deleting both elements (construct ΔSL1-ΔSL3) reduced packaging to 5%. Because SL1 and SL3 each contain at least one Gag interaction site (10), this finding is consistent with the view that Gag binding to these sites is a major determinant of encapsidation.

We investigated the structural requirements for genomic encapsidation activity in SL1 and SL3 by reinserting mutant forms of these elements into the ΔSL1 and ΔSL3 deletants (Fig. 1C). In general, mutations in SL3 were better tolerated than those in SL1. Thus, an SL3 variant in which all bases of the 5′ strand of the putative stem were mutated to prevent base pairing (construct dS.3) reduced genomic packaging to 42% of the wild-type level, but packaging efficiency was fully restored in a second variant (mS.3) with compensatory 3′-strand mutations that could restore stem formation. A transition mutation of all four bases in the putative SL3 loop region likewise had only a minimal effect on encapsidation (construct AAGA.3). These results indicate that the structure of the SL3 stem contributes to packaging but that the specific sequences of the stem and loop do not. As expected, reinserting the wild-type SL1 sequence into ΔSL1 restored genomic packaging to nearly wild-type levels (construct wt). Mutations that disrupted the proposed base-pairing pattern in the stem of SL1 (construct dS.1) markedly inhibited packaging, whereas compensatory mutations predicted to restore base-pairing (construct mS.1) restored packaging to roughly 40% of the wild-type level. The genomic content was severely impaired in two mutants in which the predicted 3-base single-stranded bulge in SL1 was either deleted (ΔB.1) or mutated (mB.1). It thus appeared that both the stem structure and the bulge sequence of SL1 were functionally required. We also tested two constructs that carried alterations in the predicted SL1 loop: the loop palindrome in one had a single point mutation (construct GCGCUC), and the loop palindrome in the other was replaced by six G residues (construct G-loop). Although these last two mutations each abolish the dimerization of HIV-1 ψ RNA in vitro (11), they had only modest effects on encapsidation. Indeed, the G-loop mutant was encapsidated at 82% of wild-type efficiency, implying that the SL1 loop palindrome was not critical for genomic packaging in virions.

The nuclease protection data also revealed that mutant virions which packaged reduced amounts of genomic transcripts tended to incorporate proportionately increased quantities of spliced viral RNA (Table 1; Fig. 3B). The ratio of genomic to spliced RNA mass within virions ranged from 10:1 for parental HIV-gpt down to 0.4:1 for ΔSL1/ΔSL3, and correlated closely with genomic packaging efficiency expressed as a percentage of the wild-type level (Table 1; Fig. 4A). This enhanced incorporation of spliced viral transcripts appeared at least partially sequence specific, in that virions from both HIV-gpt and ΔSL1/ΔSL3 each incorporated only trace amounts of four cellular RNAs (β-actin, cyclophilin, and glyceraldehyde 6-phosphate dehydrogenase mRNAs and 28S rRNA), as measured by the nuclease protection assay on virion-derived RNA (data not shown).

The infectivity of the various mutants was then quantified by their ability to induce gpt^+ colony formation in cultured HOS

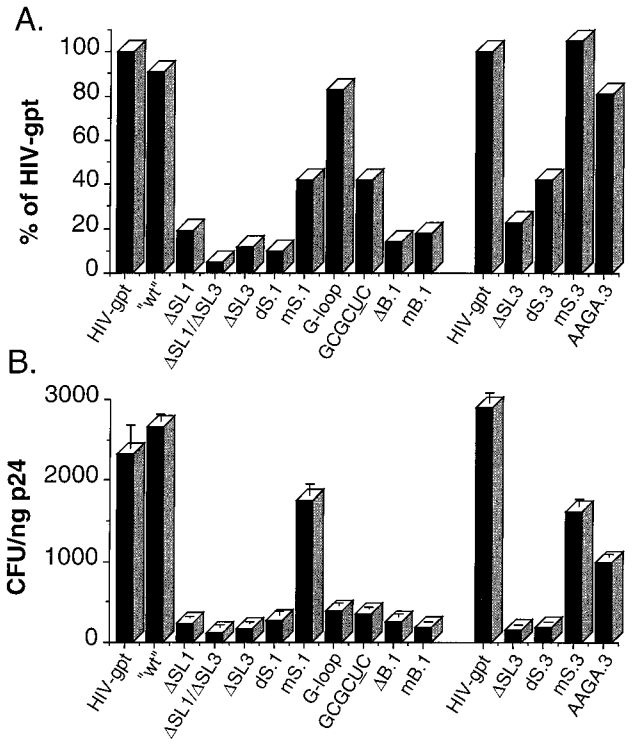

FIG. 4. Quantitation of RNA packaging efficiencies versus viral infectivities. (A) The amount of genomic RNA packaged in each mutant was compared to that in the parental HIV-gpt virus after quantitation of the genomic bands derived from the RNase protection assays by PhosphorImager analysis. Two representative experiments are shown on the right and left of the graph. (B) Infectivities of the constructs expressed as the *gpt*$^+$ CFU per nanogram of the viral antigen p24. Two representative experiments are shown on the right and left of the graph. Assays of viral stocks from at least three independent transfection and infection assays yielded similar results.

cells (Table 1; Fig. 4B). Not surprisingly, we found that mutants that were defective in genomic encapsidation (Fig. 4A) exhibited correspondingly severe defects in infectivity (Fig. 4B) and that most mutants with intact encapsidation function had infectivities approaching that of the parental virus. The only notable exceptions were the two mutants involving the SL1 loop palindrome (G-loop and GCGCUC), both of which showed infectivity defects that were out of proportion to their modest deficits in encapsidation. The G-loop mutant virions, in particular, had reduced infectivity despite a nearly normal content of genomic RNA. In light of the known inability of these mutant RNAs to dimerize in vitro, this finding suggested that genomic dimerization makes a significant contribution to viral infectivity even though it appears dispensable for encapsidation.

To ascertain whether certain mutations in SL1 did affect the dimerization state of HIV-1 RNA in vivo, RNA was isolated from gently deproteinated virions of HIV-gpt, mS.1, dS.1, and ΔSL1; this virion-derived RNA was then preheated to various temperatures for 10 min and analyzed by nondenaturing gel electrophoresis. As shown in Fig. 5, we found that at temperatures up to 40°C, RNA from HIV-gpt (Fig. 5A and B) and mS.1 (Fig. 5B) migrated as a single predominant band, which presumably represented a genomic dimer. When preheated to progressively higher temperatures, these dimers dissociated to apparent monomers (as well as to heterogeneous smaller species that probably result from RNA nicking in the virion). The melting temperature of the HIV-gpt or mS.1 dimers was approximately 50 to 55°C, a value consistent with those reported for HIV-1 and other retroviruses (14, 15). By contrast, dS.1 and ΔSL1 virion-derived RNAs migrated quite heterogeneously and contained elevated amounts of monomer-sized RNA species, even at 25 to 40°C. RNAs from dS.1 and ΔSL1 virions also contained discrete bands, other than the monomers, which were visible above 55°C, migrated around the 1.9-kb marker, and presumably represent the aberrantly packaged spliced RNAs identified earlier by the RNase protection assay. The melting temperatures of the heterogeneous RNA species isolated from these mutants was similar to that of the wild-type dimer (Fig. 5). These findings support the view that the absence of a properly folded SL1 element leads to reduced or aberrant formation or maintenance of genomic RNA dimers in HIV-1 virions.

DISCUSSION

The results of this study and of others published recently (5, 18, 28) provide in vivo support for our working model (10) of the organization of HIV-1 ψ RNA, as well as for the concept that Gag-ψ interactions are critical for HIV-1 encapsidation. In particular, we find that two of the predicted stem-loops in ψ (SL1 and SL3), each of which contains at least one independent, high-affinity binding site for Gag protein in vitro, both contribute to RNA packaging in vivo. Deletion or mutation of either of these elements alone resulted in significant packaging deficits, and deletion of both reduced the genomic content of virions by 95%. It is not clear to what extent the residual 5% packaging of the double-deletant ΔSL1/ΔSL3 indicates residual ψ activity in SL4 and elsewhere or is simply an irreducible background due to the high-level proviral expression in our packaging system. In agreement with another study (28), we find that the activities of SL1 and SL3 are inhibited by mutations that disrupt base pairing in their stems but are preserved when complementary mutations restore stem formation. This implies that the folded structures, but not the specific sequences, of SL1 and SL3 are required for activity and serves as genetic evidence that these structures form and are functionally relevant in vivo.

Although the mutations we introduced into the presumed loop regions of SL1 and SL3 had little effect on genomic packaging, those targeting the 3-base bulge of SL1 (i.e., ΔB.1 and mB.1) were notably more deleterious. This suggests that the bulge may contribute to SL1 recognition and binding by Gag and hence to encapsidation. We note, in this regard, that two of the three ψ stem-loops with the highest affinity for Gag (SL3 and SL4) each include 4-base loops composed only of purines, while the third (SL1) includes a 3-base purine bulge and a loop in which purines predominate. In light of the apparent preference of Gag for binding to purine-rich sequences (10), it is possible that these features contribute disproportionately to Gag binding. Consistent with this view, mutations in our series which preserved or increased the purine content at these sites (constructs G-loop and AAGA.3) had only minor effects on packaging.

Previously, it has been shown that mutations in the SL3 region lead to increased encapsidation of spliced viral RNAs (25, 28). We found that mutant virions with decreased genomic RNA contents tended to package correspondingly increased amounts of spliced viral RNA whether the mutations were in SL1 and/or in SL3 (Table 1; Fig. 3B). The close inverse relationship between these two parameters suggests that spliced RNA may be encapsidated by the mutants in quantities sufficient to fill space normally occupied by genomic transcripts. These data show that spliced transcripts of the mutants ΔSL1

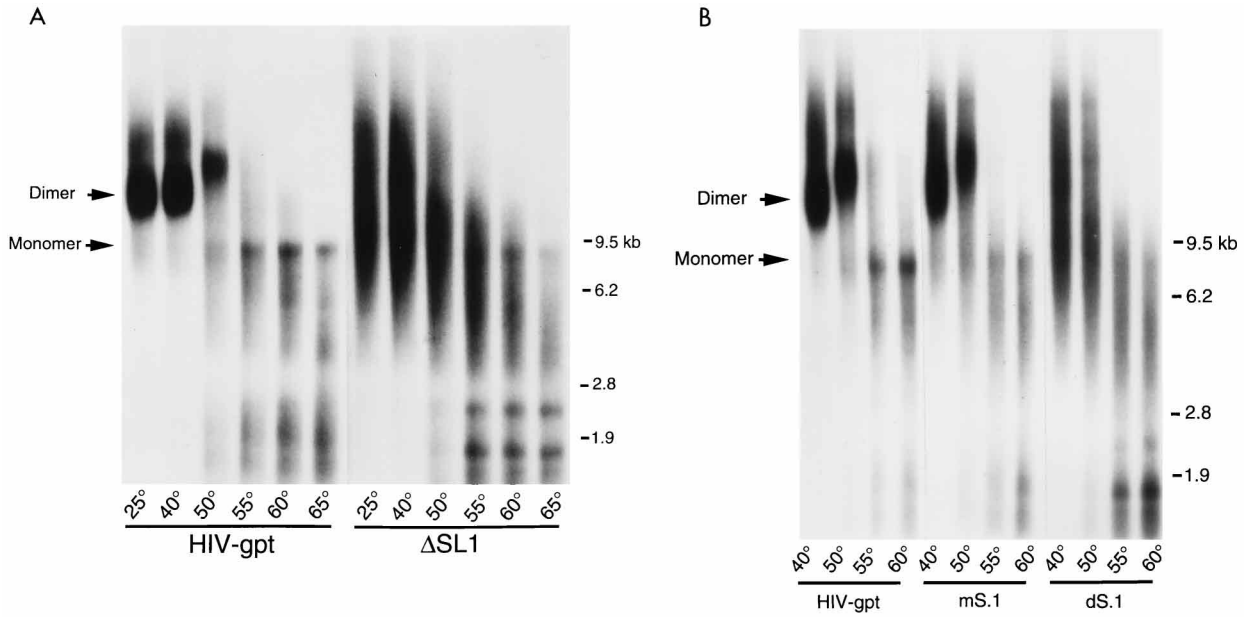

FIG. 5. Nondenaturing Northern blots of virion-derived RNA. (A) RNA extracted from pelleted HIV-gpt or ΔSL1 virions was heated to the indicated temperatures for 10 min prior to electrophoresis on 1% agarose gels at 4°C. (B) RNA extracted from HIV-gpt, mS.1, or dS.1 virions was subjected to electrophoresis and blotting as described above and in Materials and Methods.

or ΔSL1/ΔSL3 are packaged relatively efficiently in our system (Fig. 3B), even though they lack essentially all elements of the defined ψ locus by virtue of the mutations they carry and excision of the *gag-pol* intron. This could perhaps be accounted for by nonspecific packaging of these highly expressed transcripts in the absence of competition by ψ-containing RNAs, although we have failed to detect significant packaging of several abundant cellular RNAs of various lengths under these conditions (data not shown). To the extent that such packaging is specific, it may indicate the presence of additional encapsidation signals elsewhere in the spliced transcripts. Candidates for such activity might include the Gag binding site which we detected—but did not precisely map—immediately upstream of SL1 (10), sequences at the extreme 5′ end of the viral RNA (16), or other, as yet unidentified sites in the leader sequence or the 3′ half of the genome.

Some mutants in our series shed light on the mechanism and biological significance of HIV-1 RNA dimerization. In particular, we tested four different mutations in the SL1 element that would be expected to interfere with the hypothesized kissing-loop interaction between RNA strands (23, 27, 32, 35) and which were each known to abolish HIV-1 ψ dimerization in vitro (11). Two of those mutants (G-loop and GCGCUC) exhibited fairly high genomic contents, suggesting that the kissing-loop interaction is not required for efficient encapsidation. The others (dS.1 and ΔSL1) had a significant packaging defect that was probably attributable to the loss of Gag binding at SL1; however, RNA gently extracted from native dS.1 or ΔSL1 virions was found to contain elevated amounts of monomer-sized species compared to wild-type virions, supporting a critical role for SL1 during genomic RNA dimerization (Fig. 5). Recently, other groups have published analyses of HIV-1 virions containing mutations that disrupt the palindromic SL1 loop (5, 18); one reported a modest increase in the amount of monomeric RNA in mutant virions (18), while the other observed no increase in monomer content but saw a decrease in the overall packaging efficiency (5). Both noted a decrease in the replication kinetics of their mutants, but neither saw a substantial difference in the melting temperature of the dimers of the mutants compared to the wild type. This agrees with our results obtained with the dS.1 and ΔSL1 mutants and suggests that interstrand base pairing in the SL1 region contributes little to the overall stability of mature virion-derived RNA multimers, at least in terms of melting temperature. Our analysis does not reveal whether individual dS.1 or ΔSL1 virions contain a single copy of the genome but suggests that at least some of the species we observed in these mutants might represent aberrant heterodimers containing both spliced and unspliced viral RNAs. In any event, the heterogeneous nature of the multimers isolated from dS.1 and ΔSL1 virions strongly suggests that HIV-1 RNAs need not be genomic dimers in order to be packageable. Moreover, both the G-loop and GCGCUC mutants showed defects in infectivity which could not be accounted for by deficiencies in genomic RNA: this was most apparent for the G-loop mutant, which retained more than 80% of wild-type packaging activity yet had impaired infectivity. This suggests that mutants lacking a functional SL1, although able to encapsidate genomes, are defective in some later step in their life cycle which depends upon genomic dimerization. In fact, after this work was submitted for review, another group reported that the RNA element we refer to as SL1 has at least two functions: one required for encapsidation and the other required for proviral DNA synthesis (31). Taken together, however, these findings offer compelling evidence that accurate genomic dimerization, initiated by SL1, is required for optimal infectivity of HIV-1 virions.

ACKNOWLEDGMENTS

We thank S. Hughes for enlightening discussions, and we thank A. Leavitt, N. Alesandro, and Z. Mosquera for technical advice and assistance.

This work was supported by a New Investigator award from the University of California AIDS Task Force (to J.C.) and by NIH grants AI-29313, AI-36636, and AI-40317.

REFERENCES

1. **Aldovini, A., and R. A. Young.** 1990. Mutations of RNA and protein sequences involved in human immunodeficiency virus type 1 packaging result in production of noninfectious virus. J. Virol. **64:**1920–1926.
2. **Baudin, F., R. Marquet, C. Isel, J. L. Darlix, B. Ehresmann, and C. Ehresmann.** 1993. Functional sites in the 5′ region of human immunodeficiency virus type 1 RNA form defined structural domains. J. Mol. Biol. **229:**382–397.
3. **Bender, W., Y. H. Chien, S. Chattopadhyay, P. K. Vogt, M. B. Gardner, and N. Davidson.** 1978. High-molecular-weight RNAs of AKR, NZB, and wild mouse viruses and avian reticuloendotheliosis virus all have similar dimer structures. J. Virol. **25:**888–896.
4. **Bender, W., and N. Davidson.** 1976. Mapping of poly (A) sequences in the electron microscope reveals unusual structure of type C oncornavirus RNA molecules. Cell **7:**595–607.
5. **Berkhout, B., and J. L. B. van Wamel.** 1996. Role of the DIS hairpin in replication of human immunodeficiency virus type 1. J. Virol. **70:**6723–6732.
6. **Berkowitz, R., J. Fisher, and S. P. Goff.** 1996. RNA packaging. Curr. Top. Microbiol. Immunol. **214:**177–218.
7. **Berkowitz, R. D., and S. P. Goff.** 1994. Analysis of binding elements in the human immunodeficiency virus type 1 genomic RNA and nucleocapsid protein. Virology **202:**233–246.
8. **Berkowitz, R. D., J. Luban, and S. P. Goff.** 1993. Specific binding of human immunodeficiency virus type 1 gag polyprotein and nucleocapsid protein to viral RNAs detected by RNA mobility shift assays. J. Virol. **67:**7190–7200.
9. **Berkowitz, R. D., A. Ohagen, S. Hoglund, and S. P. Goff.** 1995. Retroviral nucleocapsid domains mediate the specific recognition of genomic viral RNAs by chimeric Gag polyproteins during RNA packaging in vivo. J. Virol. **69:**6445–6456.
10. **Clever, J., C. Sassetti, and T. G. Parslow.** 1995. RNA secondary structure and binding sites for *gag* gene products in the 5′ packaging signal of human immunodeficiency virus type 1. J. Virol. **69:**2101–2109.
11. **Clever, J. L., M. L. Wong, and T. G. Parslow.** 1996. Requirements for kissing-loop-mediated dimerization of human immunodeficiency virus RNA. J. Virol. **70:**5902–5908.
12. **Darlix, J. L., C. Gabus, M. T. Nugeyre, F. Clavel, and S. F. Barre.** 1990. Cis elements and trans-acting factors involved in the RNA dimerization of the human immunodeficiency virus HIV-1. J. Mol. Biol. **216:**689–699.
13. **Dorfman, T., J. Luban, S. P. Goff, W. A. Haseltine, and H. G. Gottlinger.** 1993. Mapping of functionally important residues of a cysteine-histidine box in the human immunodeficiency virus type 1 nucleocapsid protein. J. Virol. **67:**6159–6169.
14. **Fu, W., R. J. Gorelick, and A. Rein.** 1994. Characterization of human immunodeficiency virus type 1 dimeric RNA from wild-type and protease-defective virions. J. Virol. **68:**5013–5018.
15. **Fu, W., and A. Rein.** 1993. Maturation of dimeric viral RNA of Moloney murine leukemia virus. J. Virol. **67:**5443–5449.
16. **Geigenmuller, U., and M. L. Linial.** 1996. Specific binding of human immunodeficiency virus type 1 (HIV-1) Gag-derived proteins to a 5′ HIV-1 genomic RNA sequence. J. Virol. **70:**667–671.
17. **Gorelick, R. J., D. J. Chabot, A. Rein, L. E. Henderson, and L. O. Arthur.** 1993. The two zinc fingers in the human immunodeficiency virus type 1 nucleocapsid protein are not functionally equivalent. J. Virol. **67:**4027–4036.
18. **Haddrick, M., A. L. Lear, A. J. Cann, and S. Heaphy.** 1996. Evidence that a kissing loop structure facilitates genomic RNA dimerisation in HIV-1. J. Mol. Biol. **259:**58–68.
19. **Harrison, G. P., and A. M. Lever.** 1992. The human immunodeficiency virus type 1 packaging signal and major splice donor region have a conserved stable secondary structure. J. Virol. **66:**4144–4153.
20. **Kim, H. J., K. Lee, and J. J. O'Rear.** 1994. A short sequence upstream of the 5′ major splice site is important for encapsidation of HIV-1 genomic RNA. Virology **198:**336–340.
21. **Kunkel, T. A.** 1985. Rapid and efficient site-specific mutagenesis without phenotypic selection. Proc. Natl. Acad. Sci. USA **82:**488–492.
22. **Landau, N. R., K. A. Page, and D. R. Littman.** 1991. Pseudotyping with human T-cell leukemia virus type I broadens the human immunodeficiency virus host range. J. Virol. **65:**162–169.
23. **Laughrea, M., and L. Jette.** 1994. A 19-nucleotide sequence upstream of the 5′ major splice donor is part of the dimerization domain of human immunodeficiency virus 1 genomic RNA. Biochemistry **33:**13464–13474.
24. **Lever, A., H. Gottlinger, W. Haseltine, and J. Sodroski.** 1989. Identification of a sequence required for efficient packaging of human immunodeficiency virus type 1 RNA into virions. J. Virol. **63:**4085–4087.
25. **Luban, J., and S. P. Goff.** 1994. Mutational analysis of *cis*-acting packaging signals in human immunodeficiency virus type 1 RNA. J. Virol. **68:**3784–3793.
26. **Marquet, R., F. Baudin, C. Gabus, J. L. Darlix, M. Mougel, C. Ehresmann, and B. Ehresmann.** 1991. Dimerization of human immunodeficiency virus (type 1) RNA: stimulation by cations and possible mechanism. Nucleic Acids Res. **19:**2349–2357.
27. **Marquet, R., J. C. Paillart, E. Skripkin, C. Ehresmann, and B. Ehresmann.** 1994. Dimerization of human immunodeficiency virus type 1 RNA involves sequences located upstream of the splice donor site. Nucleic Acids Res. **22:**145–151.
28. **McBride, M. S., and A. T. Panganiban.** 1996. The human immunodeficiency virus type 1 encapsidation site is a multipartite RNA element composed of functional hairpin structures. J. Virol. **70:**2963–2973.
29. **Murti, K. G., M. Bondurant, and A. Tereba.** 1981. Secondary structural features in the 70S RNAs of Moloney murine leukemia and Rous sarcoma viruses as observed by electron microscopy. J. Virol. **37:**411–419.
30. **Page, K. A., N. R. Landau, and D. R. Littman.** 1990. Construction and use of a human immunodeficiency virus vector for analysis of virus infectivity. J. Virol. **64:**5270–5276.
31. **Paillart, J. C., L. Berthoux, M. Ottman, J. L. Darlix, R. Marquet, B. Ehresmann, and C. Ehresmann.** 1996. A dual role of the putative RNA dimerization initiation site of human immunodeficiency virus type 1 in genomic RNA packaging and proviral DNA synthesis. J. Virol. **70:**8348–8354.
32. **Paillart, J. C., R. Marquet, E. Skripkin, B. Ehresmann, and C. Ehresmann.** 1994. Mutational analysis of the bipartite dimer linkage structure of human immunodeficiency virus type 1 genomic RNA. J. Biol. Chem. **269:**27486–27493.
33. **Poon, D. T. K., J. Wu, and A. Aldovini.** 1996. Charged amino acid residues of human immunodeficiency virus type 1 nucleocapsid p7 protein involved in RNA packaging and infectivity. J. Virol. **70:**6607–6616.
34. **Sakaguchi, K., N. Zambrano, E. T. Baldwin, B. A. Shapiro, J. W. Erickson, J. G. Omichinski, G. M. Clore, A. M. Gronenborn, and E. Appella.** 1993. Identification of a binding site for the human immunodeficiency virus type 1 nucleocapsid protein. Proc. Natl. Acad. Sci. USA **90:**5219–5223.
35. **Skripkin, E., J. C. Paillart, R. Marquet, B. Ehresmann, and C. Ehresmann.** 1994. Identification of the primary site of the human immunodeficiency virus type 1 RNA dimerization in vitro. Proc. Natl. Acad. Sci. USA **91:**4945–4949.
36. **Weiss, S., B. Konig, Y. Morikawa, and I. Jones.** 1992. Recombinant HIV-1 nucleocapsid protein p15 produced as a fusion protein with glutathione S-transferase in Escherichia coli mediates dimerization and enhances reverse transcription of retroviral RNA. Gene **121:**203–212.